*Aust. J. Phys.*, 1980, **33**, 539–47

# A Study of Centre-fed Antiphase Circular Antennas in a Warm Plasma

*K. R. Soni and C. L. Arora*

Department of Physics, Malaviya Regional Engineering College, Jaipur 302 004, India.

*Abstract*

The radiation characteristics of a centre-fed antiphase circular arc antenna immersed in a warm electron plasma are studied using linearized hydrodynamic theory. The effects of antenna and plasma parameters on the radiation properties have been studied by computing the results and presenting them graphically. It is found that, whereas the power radiated in the TEM mode depends on the length as well as on the angle of the arc antenna, the power in the LP mode is independent of the angle and depends only on the length of the arc. It is also found that the power in the LP mode is relatively much larger in the case of small angled centre-fed antiphase arc antennas. Hence small angled arcs should be suitable for the launching of plasma waves, whereas large angled arcs will be more useful for communication through a plasma medium.

## Introduction

Most of the previous theoretical studies on the radiation properties of different radiating sources in a plasma have been carried out following the vector potential method and using the linearized hydrodynamic theory of plasmas. The majority of these investigations have been concerned with linear antennas, especially dipoles, and comparatively few have dealt with nonlinear configurations. However, the latter types of antennas have been considered in our recent investigations on end-fed travelling wave and centre-fed, in-phase, standing-wave circular arc antennas (Soni and Arora 1979*a*, 1979*b*). In these studies we have determined the dependence of the radiation properties of the antenna on its length as well as on its curvature.

The present work is aimed at extending the above studies on circular arcs to the case of a centre-fed, antiphase, standing-wave arc antenna and at developing general expressions for its radiation fields and resistance. This type of arc antenna has not been studied previously, although some information does exist for the antiphase standing-wave linear antenna (Freeston and Gupta 1973), which has been suggested as possibly suitable for the launching of plasma waves.

## Radiation Fields of the Arcs

The plasma is assumed to be warm, homogeneous, isotropic and neutral in its unperturbed state. Perturbations due to the source are taken to be small with an exponential time dependence $\exp(j\omega t)$. The electrons are assumed to be the only effective components of the plasma, the ions being a stationary neutralizing background. Collisions of the electrons are neglected. A circular arc antenna of radius $a$ and angle $\phi_0$, as shown in Fig. 1, is embedded in the plasma. It is symmetrically fed at $\phi = \phi' = 0°$ with the currents in its two halves being of the same magnitude but of opposite phases. Thus the assumed current distribution on the antenna can be expressed as

$$I_1(\phi') = I_m \sin\{\beta a(\tfrac{1}{2}\phi_0 - \phi')\} \exp(j\omega t), \tag{1a}$$

$$I_2(\phi') = I_m \sin\{\beta a(\tfrac{1}{2}\phi_0 + \phi')\} \exp\{j(\omega t + \pi)\}$$
$$= -I_m \sin\{\beta a(\tfrac{1}{2}\phi_0 + \phi')\} \exp(j\omega t), \tag{1b}$$

where $I_1(\phi')$ and $I_2(\phi')$ are the currents in the two halves of the arc, $I_m$ is the maximum current and $\beta$ is the phase propagation constant of the current wave.

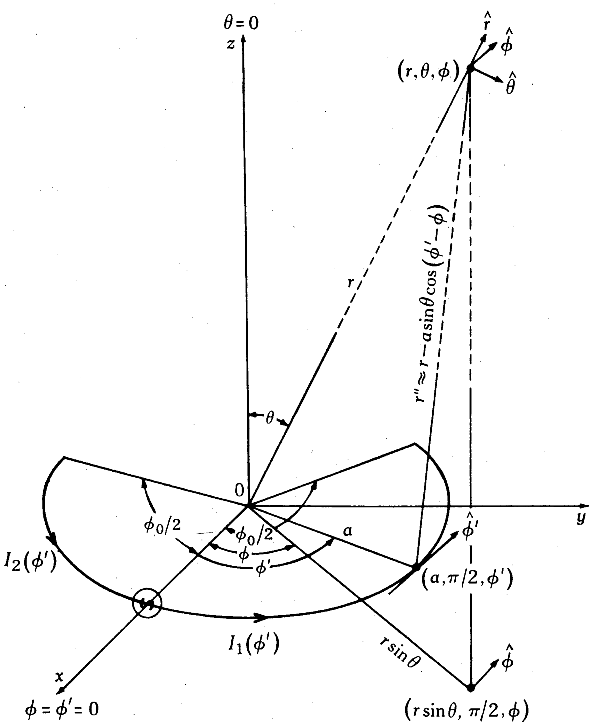


**Fig. 1.** Geometry of orientation of a centre-fed, antiphase standing-wave circular arc antenna in a spherical coordinate system.

By using the basic equations given by Soni and Arora (1979) we can write down the expressions for the transverse electromagnetic (TEM) and longitudinal plasma (LP) mode components of the electric field $\boldsymbol{E}$ as follows. For the TEM mode field we have

$$E_{e\theta} = E_0 \cos\theta \left( \int_0^{\frac{1}{2}\phi_0} \sin(\phi' - \phi) \sin\{\beta a(\tfrac{1}{2}\phi_0 - \phi')\} f_1 \, d\phi' - \int_{-\frac{1}{2}\phi_0}^{0} \sin(\phi' - \phi) \sin\{\beta a(\tfrac{1}{2}\phi_0 + \phi')\} f_1 \, d\phi' \right), \tag{2a}$$

$$E_{e\phi} = -E_0\left(\int_0^{\frac{1}{2}\phi_0} \cos(\phi'-\phi)\sin\{\beta a(\tfrac{1}{2}\phi_0-\phi')\} f_1 \, d\phi' - \int_{-\frac{1}{2}\phi_0}^{0} \cos(\phi'-\phi)\sin\{\beta a(\tfrac{1}{2}\phi_0+\phi')\} f_1 \, d\phi'\right), \tag{2b}$$

where

$$E_0 = j(ZI_m/4\pi r)\beta_e a \exp(-j\beta_e r), \tag{3a}$$

$$f_1 = \exp\{j\beta_e a \sin\theta \cos(\phi'-\phi)\}, \tag{3b}$$

with $Z$ the intrinsic impedance of the plasma medium, $\beta_e$ the phase propagation constant of electromagnetic waves in the plasma and $(r, \theta, \phi)$ the spherical coordinates of a space point. Similarly, for the LP mode field we have

$$E_{pr} = -E_{p0}\left(\int_0^{\frac{1}{2}\phi_0} \cos\{\beta a(\tfrac{1}{2}\phi_0-\phi')\} f_2 \, d\phi' - \int_{-\frac{1}{2}\phi_0}^{0} \cos\{\beta a(\tfrac{1}{2}\phi_0+\phi')\}\exp(j\pi) f_2 \, d\phi'\right), \tag{4}$$

where

$$E_{p0} = (ZI_m/4\pi r)\beta_p a(\beta/\beta_e)(\omega_p/\omega)^2 \exp(-j\beta_p r), \tag{5a}$$

$$f_2 = \exp\{j\beta_p a \sin\theta \cos(\phi'-\phi)\}, \tag{5b}$$

with $\beta_p$ the phase propagation constant of the plasma mode, $\omega_p$ the angular plasma frequency of the electrons and $\omega$ the angular frequency of the antenna.

The solutions of the foregoing integrals can be obtained by using a method similar to that given by Talekar and Soni (1973), and after some mathematical manipulation the expressions for the components of the electric intensity finally become:

$$E_{e\theta} = -j(4E_0/\beta_e a)\cot\theta \sum_{q=1}^{\infty} j^q q J_q(\beta_e a \sin\theta) f_3(q, \beta a, \phi_0)\cos(q\phi), \tag{6a}$$

$$E_{e\phi} = -4E_0 \sum_{q=1}^{\infty} j^q J_q'(\beta_e a \sin\theta) f_3(q, \beta a, \phi_0)\sin(q\phi), \tag{6b}$$

$$E_{pr} = -4E_{p0}\left(\tfrac{1}{2}J_0(\beta_p a \sin\theta) f_4(0, \beta a, \phi_0) + \sum_{q=1}^{\infty} j^q J_q(\beta_p a \sin\theta) f_4(q, \beta a, \phi_0)\cos(q\phi)\right), \tag{6c}$$

where

$$f_3(q, \beta a, \phi_0) = (\beta^2 a^2 - q^2)^{-1}\{\beta a \sin(\tfrac{1}{2}q\phi_0) - q\sin(\tfrac{1}{2}\beta a\phi_0)\}, \tag{7a}$$

$$f_4(q, \beta a, \phi_0) = (\beta^2 a^2 - q^2)^{-1}\{\beta a \sin(\tfrac{1}{2}\beta a\phi_0) - q\sin(\tfrac{1}{2}q\phi_0)\} \tag{7b}$$

and $J_q(x)$ is a Bessel function of the first kind, with $J_q'(x)$ its derivative.

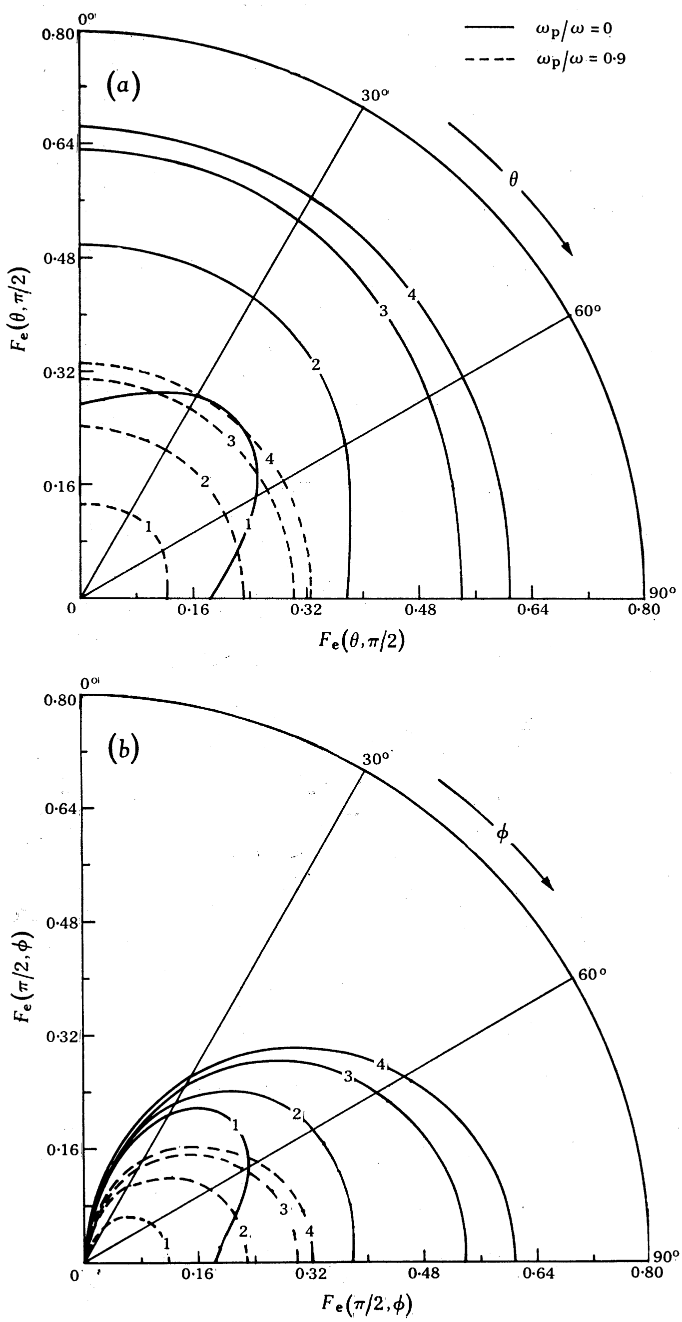


**Fig. 2.** Angular variation of the far-field pattern factors $F_e$ for half-wave ($S_{\lambda_0} = 0{\cdot}5$) centre-fed, antiphase standing-wave circular arc and loop antennas in the (*a*) $\phi = \frac{1}{2}\pi$ and (*b*) $\theta = \frac{1}{2}\pi$ planes. The radiation fields are compared for the antennas in plasma and in free space, with the normalized plasma frequency $\omega_p/\omega = 0{\cdot}9$ and 0 respectively. For ease of labelling, the curves are identified by the $\phi_0$ value of the antenna in units of $\frac{1}{2}\pi$ (e.g. curve 4 is for $\phi_0 = 2\pi$).

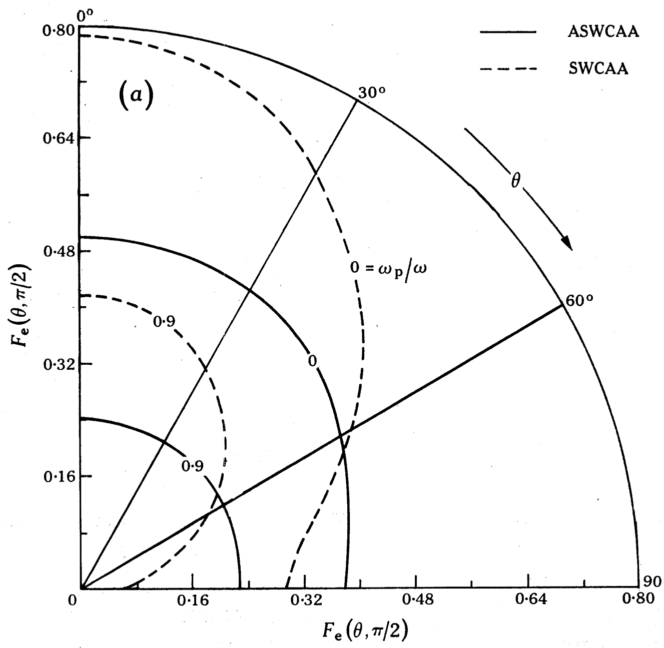


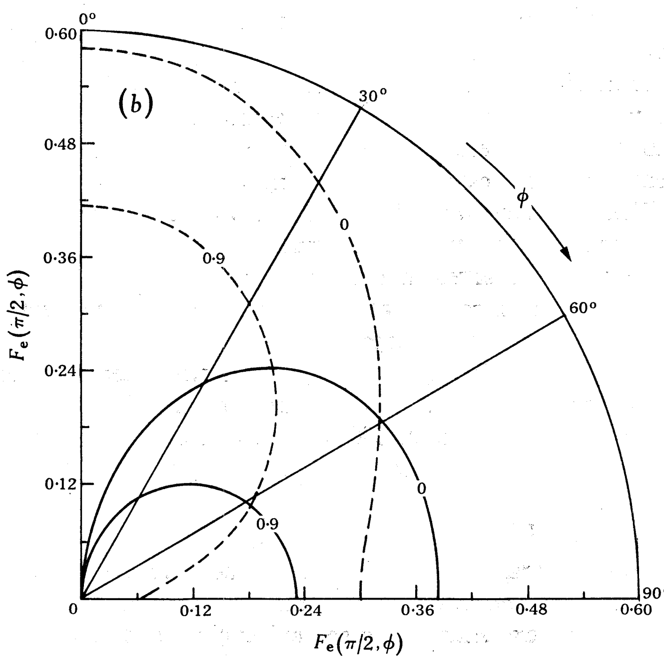


**Fig. 3.** Angular variation of the far-field pattern factors $F_e$ for half-wave ($S_{\lambda_0} = 0\cdot5$) centre-fed, antiphase and in-phase standing-wave semicircular ($\phi_0 = \pi$) arc antennas (ASWCAA and SWCAA respectively) in the (*a*) $\phi = \frac{1}{2}\pi$ and (*b*) $\theta = \frac{1}{2}\pi$ planes. The radiation fields are compared for the antennas in plasma and in free space ($\omega_p/\omega = 0\cdot9$ and 0 respectively).

The TEM mode electric intensity $\boldsymbol{E}_e$ is related to the field pattern factor $F_e$ by the definition

$$F_e(\theta,\phi) = (2\pi r/Z_0 I_m)\,|\boldsymbol{E}_e|\,, \tag{8}$$

where $Z_0$ is the intrinsic impedance of free space. In the $\phi = \frac{1}{2}\pi$ and $\theta = \frac{1}{2}\pi$ planes, the pattern factors $F_e(\theta,\frac{1}{2}\pi)$ and $F_e(\frac{1}{2}\pi,\phi)$ have been evaluated here for three half-wave arcs of the same normalized length given by $S_{\lambda_0} = a\phi_0/\lambda_0 = 0\cdot 5$ ($\lambda_0$ being the wavelength of electromagnetic waves in free space) but of different curvatures corresponding to $\phi_0$ values of $\frac{1}{2}\pi$ (quarter circular), $\pi$ (semicircular) and $\frac{3}{2}\pi$ (three-quarter circular). Calculations have also been performed for a centre-fed, antiphase standing-wave open loop antenna ($\phi_0 = 2\pi$) of normalized circumference $C_{\lambda_0} = 2\pi a/\lambda_0 = 0\cdot 5$. For all the calculations $\beta$ was set equal to $\beta_e$, a suitable value suggested by previous experimental as well as theoretical studies on antennas in plasma (Judson *et al.* 1968; Gupta and Freeston 1970).

The spatial distribution of the radiation fields in a plasma of the antennas described above has been compared with that of the antennas in free space by calculating the pattern factors $F_e$ for two values of the normalized plasma frequency, namely $\omega_p/\omega = 0\cdot 9$ (plasma frequency near that of the antenna) and $\omega_p/\omega = 0$ (free space), and the results are presented graphically in Fig. 2. In order to compare the performance of an antiphase standing-wave circular arc antenna (ASWCAA) with that of an in-phase standing-wave circular arc antenna (SWCAA), the field pattern factors for both types of arcs are plotted in Fig. 3 for a semicircular arc of normalized length $S_{\lambda_0} = 0\cdot 5$ in plasma ($\omega_p/\omega = 0\cdot 9$) and in free space ($\omega_p/\omega = 0$).

It is evident from Fig. 2 that the field distribution of an ASWCAA is in the form of a limited number of wide lobes of large beamwidth. The presence of plasma surrounding the antenna decreases the magnitude of its free-space radiation intensity to a great extent. In these respects the performance of an ASWCAA is similar to that of an SWCAA. However, Fig. 2 also shows the characteristic points of dissimilarity between the two types of antennas. From the graphs and also from the calculated values it is observed that for an ASWCAA of given length the electric intensity in any direction increases with the antenna curvature, while the reverse is true for an SWCAA in most of space.

Fig. 3 indicates that the magnitude of the electric intensity radiated by an ASWCAA is, in general, less than that radiated by an SWCAA when operating under similar conditions. Unlike an SWCAA, the electric intensity radiated by an ASWCAA along its axis is always zero.

## Radiation Resistances of the Arcs

Expressions for the components $R_e$ and $R_p$ of radiation resistance pertaining to TEM and LP modes respectively can be obtained from the expressions for the components of the far-zone fields using the well-known relations

$$R_e = \frac{1}{ZI_m^2}\int_{\theta=0}^{\pi}\int_{\phi=0}^{2\pi}(|E_{e\theta}|^2+|E_{e\phi}|^2)\,r^2\sin\theta\,d\theta\,d\phi\,, \tag{9a}$$

$$R_p = \frac{1}{ZI_m^2}\frac{u\omega^2}{c\omega_p^2}\int_{\theta=0}^{\pi}\int_{\phi=0}^{2\pi}|E_{pr}|^2 r^2\sin\theta\,d\theta\,d\phi\,. \tag{9b}$$

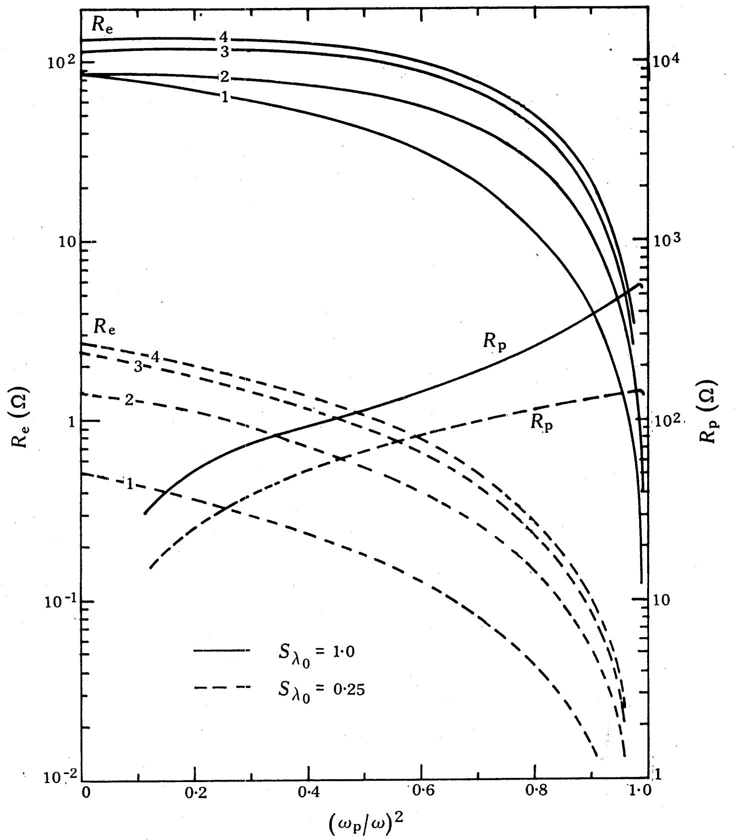


**Fig. 4.** Calculated dependences of the components $R_e$ and $R_p$ of the radiation resistance of full-wave ($S_{\lambda_0} = 1 \cdot 0$) and quarter-wave ($S_{\lambda_0} = 0 \cdot 25$) centre-fed, antiphase standing-wave circular arc and loop antennas on the square of the normalized plasma frequency $\omega_p/\omega$, taking $\beta = \beta_e$ and $c/u \geqslant 10^3$. The $R_e$ curves are labelled 1–4 in $\phi_0$ units of $\frac{1}{2}\pi$ while the $R_p$ curves apply for all four values of $\phi_0$.

After substitution in these relations from equations (6) and (7) for the components of the electric intensity and evaluation of the integrals, the following final expressions for $R_e$ and $R_p$ are obtained:

$$R_e = \frac{Z\beta_e a}{\pi} \sum_{q=0}^{\infty} J_{2q+1}(2\beta_e a) \bigg( \{f_3(q+1, \beta a, \phi_0)\}^2 - \{f_3(q, \beta a, \phi_0)\}^2 + \frac{2}{\beta_e^2 a^2} \sum_{p=0}^{q} (\beta_e^2 a^2 - p^2)\{f_3(p, \beta a, \phi_0)\}^2 \bigg), \quad (10a)$$

$$R_p = \frac{Z\beta^2 a^2}{\pi \beta_e a} \left(\frac{\omega_p}{\omega}\right)^2 \sum_{q=0}^{\infty} J_{2q+1}(2\beta_p a) \times \bigg( -\{f_4(0, \beta a, \phi_0)\}^2 + 2 \sum_{p=0}^{q} \{f_4(p, \beta a, \phi_0)\}^2 \bigg). \quad (10b)$$

The equations (10) have been used to compute $R_e$ and $R_p$ for full-wave ($S_{\lambda_0} = 1\cdot 0$) and quarter-wave ($S_{\lambda_0} = 0\cdot 25$) arc antennas for different values of $(\omega_p/\omega)^2$ ranging from 0 to 1. For each antenna length, different curvatures corresponding to $\phi_0 = \frac{1}{2}\pi$, $\pi$, $\frac{3}{2}\pi$ and $2\pi$ have been considered. Here also, $\beta$ was taken equal to $\beta_e$. The results are presented in Fig. 4. Since $R_p$ is of much higher order than $R_e$, different scales have been used to plot these quantities in the figure.

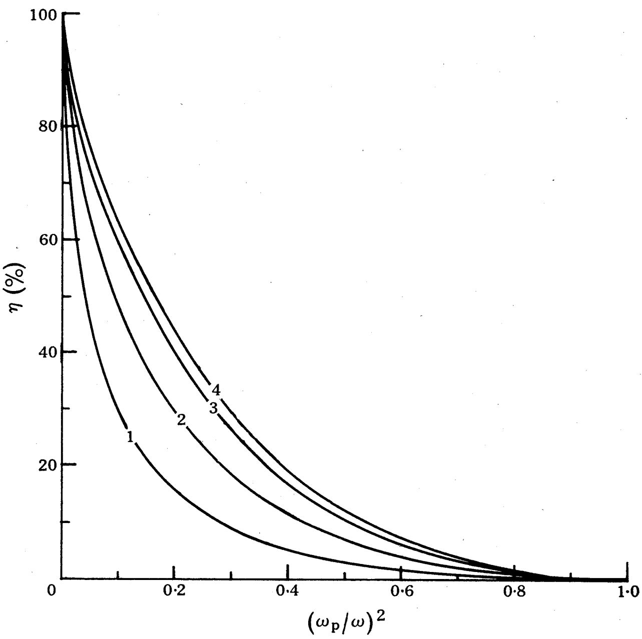


**Fig. 5.** Variation of the radiation efficiency $\eta$ of half-wave ($S_{\lambda_0} = 0\cdot 5$) centre-fed, anti-phase standing-wave circular arc and loop antennas with the square of the normalized plasma frequency $\omega_p/\omega$. The curves are labelled in $\phi_0$ units of $\frac{1}{2}\pi$.

The radiation efficiency $\eta$ of an antenna in a plasma is defined as the ratio of the power radiated in the TEM mode to the total power input, that is,

$$\eta = R_e/(R_e+R_p+R_1), \tag{11}$$

where $R_1$ is the resistance of the antenna wire, which is assumed to be negligible here. Values of $\eta$ have been calculated for arcs of length $S_{\lambda_0} = 0\cdot 5$ having $\phi_0 = \frac{1}{2}\pi$, $\pi$ and $\frac{3}{2}\pi$, along with the loop ($\phi_0 = 2\pi$) of circumference $C_{\lambda_0} = 0\cdot 5$. The results are presented in Fig. 5, where $\eta$ is plotted against $(\omega_p/\omega)^2$.

The characteristic features of Figs 4 and 5 may now be summarized. The radiation resistance $R_e$ for an arc antenna is found to depend on its length as well as on its curvature. For an ASWCAA of any given length and plasma frequency, $R_e$ increases with the curvature, which is the reverse of that observed in the case of an SWCAA. The same is true for $\eta$ also, which suggests that the efficiency of a large angled ASWCAA is always greater than that of a small angled arc. The value of $R_p$ for an ASWCAA at any plasma frequency primarily depends on its length, and it remains independent of the curvature for a given length. This feature is similar to those observed in the case of an SWCAA and an end-fed travelling wave arc antenna.

## Conclusions

From the analytical expressions developed here for the far-zone fields and radiation resistances of antiphase standing-wave arc antennas in an electron plasma, it is seen that the power radiated in the TEM mode by such an antenna depends on the length of the antenna as well as on its curvature. For an antenna of a given length and plasma frequency, this power is found to increase with the curvature. In contrast, the power radiated in the LP mode only depends on the length of the antenna. Further, it is seen that, for a small angled arc antenna, the power in the LP mode is of much higher order than that in the TEM mode. This was also found in the case of centre-fed, antiphase standing-wave linear antennas by Freeston and Gupta (1973), and they have suggested that this type of linear antenna could be used for launching plasma waves. Thus from their work on linear antennas and the present study of arc antennas, we may conclude that linear and small angled arc antennas should be suitable for the launching of plasma waves, whereas large angled arcs or loops will be more useful for communication through a plasma medium.

## Acknowledgment

This research was supported by the University Grants Commission, New Delhi, under Grant No. 8239.

## References

Freeston, I. L., and Gupta, R. K. (1973). *Int. J. Electron.* **35**(5), 659.
Gupta, R. K., and Freeston, I. L. (1970). *Electron. Lett.* **6**, 553.
Judson, H., Chen, K. M., and Lundquist, R. (1968). *Electron. Lett.* **4**, 289.
Soni, K. R., and Arora, C. L. (1979*a*). *Int. J. Electron.* **46**, 141.
Soni, K. R., and Arora, C. L. (1979*b*). *Aust. J. Phys.* **32**, 575.
Talekar, V. L., and Soni, K. R. (1973). *Int. J. Electron.* **34**(4), 497.

Manuscript received 24 May 1979, accepted 21 September 1979